Nonredundant Information Collection in Rescue Applications via an Energy-Constrained UAV

Yan Liang, Wenzheng Xu, *Member, IEEE*, Weifa Liang, *Senior Member, IEEE*, Jian Peng, Xiaohua Jia, *Fellow, IEEE*, Yingjie Zhou, *Member, IEEE*, and Lei Duan

***Abstract*—Unmanned aerial vehicles (UAVs) are emerging as promising devices to provide valuable information in rescue applications, which can be dispatched to take photographs for points of interests in disaster areas where humans are hard to approach. Most existing studies focused on the limited energy capacity issue of UAVs when they take photographs, which however ignored an important fact, that is, the photographs taken by the UAVs usually are highly redundant. In this paper we study a novel monitoring quality maximization problem to find a flying tour for an energy-constrained UAV, such that the amount of nonredundant information of the photographs taken by the UAV in its tour is maximized. Due to NP-hardness of the problem, we first propose an approximation algorithm with a quasi-polynomial time complexity. We then devise a fast yet scalable heuristic algorithm for the problem. We finally evaluate the performance of the proposed algorithms via both a real dataset and extensive simulations. Experimental results show that the proposed algorithms are very promising. Especially, the amounts of nonredundant information by the proposed approximation and heuristic algorithms are about 11% and 8% larger than that by the state-of-the-art, respectively. To the best of our knowledge, we are the first to consider the novel problem of collecting nonredundant information with an energy-constrained UAV.**

***Index Terms*—Approximation algorithms, constrained optimization, flying tour planning, nonredundant information collection, unmanned aerial vehicles (UAVs).**

I. Introduction

UNMANNED aerial vehicles (UAVs), or drones, e.g., a DJI phantom 4 Pro UAV [25], are lightweight aircrafts without a human pilot on board, which now are low-cost, robust, and commercially available. UAVs equipped with various types of sensors have many applications, such as disaster management [7], water management [3], area coverage [24], [34], urban sensing [5], [22], [23], [36], precision agriculture [12], [29], animal monitoring [39], detection of collapsed buildings [11], [20], targets tracking [14], [26], [43], charging wireless sensor networks [9], [37], [38], [40], [44], and so on.

Particularly, when a disaster (e.g., an earthquake, a hurricane, a landslide, or a flooding) occurs, the most important issue is to save human lives. It is well recognized that the first 72 h after the disaster are the most critical, and search and rescue operations should be performed very quickly and efficiently [7]. However, a major problem is the lack of situational awareness about the disaster, while transportation, and communication infrastructures for such rescues may already have been damaged. In this situation, UAVs equipped with a camera can be deployed to take photographs in the disaster area, in order to provide valuable information for rescue decisions [1], [2], [10], [19]. For example, in September 14, 2017, the hurricane Irma struck Florida. UAVs were dispatched for taking photographs in the disaster area, so as to discover people in danger, monitor levees, and measure damages [6].

Several pioneering studies have been conducted about the scheduling of camera-equipped UAVs to collect information through taking photographs or videos [19], [27], [29], [30], [35]. For example, Wang *et al.* [35] studied the problem of scheduling multiple UAVs to cover the ball and players in a football field, so as to maximize the throughput of videoed data from the UAVs to nearby servers, assuming that each UAV has an unlimited energy supply. Torres *et al.* [30] investigated the problem of dispatching a UAV to fully cover an area of interest for its 3-D terrain reconstruction so that the energy consumption of the UAV is minimized, while Scott *et al.* [27] later extended the work in [30] from a single UAV case to the multiple UAVs case.

Unlike the aforementioned studies in [27], [30], and [35] that assumed that each UAV has an unlimited energy supply for its flying, a few researchers recognized that UAVs usually are energy-constrained. For example, a fully charged DJI phantom 4 Pro UAV can fly only about 30 min [25]. Tokekar *et al.* [29] considered the problem of scheduling a UAV to maximize the number of points of interest (POI) visited, given the battery energy budget of the UAV. Mersheeva and Friedrich [19] investigated the problem of dispatching a fleet of UAVs with limited energy budgets to visit

Manuscript received August 17, 2018; revised October 10, 2018; accepted October 18, 2018. Date of publication October 23, 2018; date of current version May 8, 2019. The work of W. Xu was supported by the National Natural Science Foundation of China (NSFC) under Grant 61602330. The work of Y. Zhou was supported by the NSFC under Grant 61801315. The work of L. Duan was supported by the NSFC under Grant 61572332. This work was supported in part by the Sichuan Science and Technology Programs under Grant 2018GZ0094, Grant 2018GZDZX0010, Grant 2018GZ0093, and Grant 2017GZDZX0003, and in part by the Fundamental Research Funds for the Central Universities under Grant 20822041B4104. *(Corresponding author: Wenzheng Xu.)*

Y. Liang, W. Xu, J. Peng, Y. Zhou, and L. Duan are with the College of Computer Science, Sichuan University, Chengdu 610065, China (e-mail: liangyan19931005@163.com; wenzheng.xu3@gmail.com; jianpeng@scu.edu.cn; yjzhou09@gmail.com; leiduan@scu.edu.cn).

W. Liang is with the Research School of Computer Science, Australian National University, Canberra, ACT 2601, Australia (e-mail: wliang@cs.anu.edu.au).

X. Jia is with the Department of Computer Science, City University of Hong Kong, Hong Kong (e-mail: csjia@cityu.edu.hk).

Digital Object Identifier 10.1109/JIOT.2018.2877409

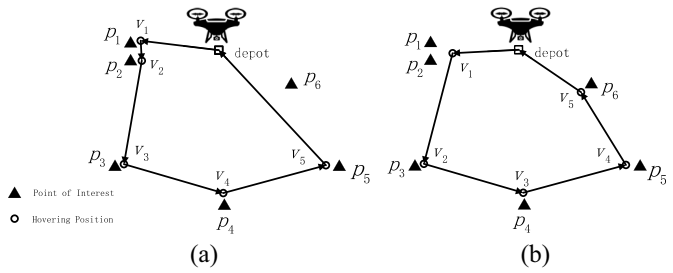

Fig. 1. There are six POIs in a disaster area, and a UAV is dispatched to monitor the six POIs. (a) Flying tour of a UAV delivered by existing studies. (b) Flying tour of a UAV when considering redundant information.

a set of POIs, so that the average number of visits of every POI is maximized for a given period.

It can be seen that although existing studies considered the problem of taking photographs for POIs while taking into account the limited energy capacities of UAVs, most of them did not consider the quality of photographs taken. That is, different photographs taken by a UAV at nearby locations usually are highly correlated with each other in terms of data. We here use an example to illustrate the photograph quality. For example, assume that there are six POIs p_1, p_2, p_3, p_4, p_5, and p_6 in a disaster area [see Fig. 1(a)], where each POI can be a school, an office building, or a mall, in which there are usually plenty of people. The geographic locations of POIs p_1 and p_2 are close to each other, while the locations of other POIs p_3, p_4, p_5, and p_6 are far away from each other. A UAV with a limited energy capacity is initially located at a depot. Existing studies dispatched the UAV to visit the maximum number of POIs, subject to the energy capacity of the UAV. Fig. 1(a) shows a flying tour of the UAV that consists of POIs p_1, p_2, p_3, p_4, and p_5, by taking photographs at each of the locations. The UAV may not be able to visit POI p_6 due to its energy capacity constraint. However, it can be seen that when the UAV takes photographs for POI p_1 at hovering position v_1, the photographs also contain valuable information for POI p_2, since POIs p_1 and p_2 are close to each other. Similarly, the photographs taken by the UAV at hovering position v_2 contain plenty of information for both POIs p_1 and p_2. In other words, the photographs taken by the UAV at v_1 and v_2 are highly information redundant. However, in a disaster rescue situation, it is very critical to collect as much nonredundant information as possible in a short time for providing valuable information for better rescue decision-making. Otherwise, people in the disaster area may be very dangerous, and the disaster loss will be unimaginable.

Unlike the aforementioned existing studies, in this paper we consider the quality information collection via a UAV that takes into account not only the limited energy capacity of the UAV but also photograph information redundancy. Fig. 1(b) shows a flying tour of the UAV. By monitoring p_1 and p_2 at the same time, the UAV can save more energy to monitor more POIs (e.g., POI p_6). In the end, the UAV can collect more valuable nonredundant information and the people trapped in a disaster area can be rescued earlier.

To this end, we study the problem of finding a flying tour for a UAV to take photographs for POIs such that the amount of nonredundant information contained in the photographs taken in the tour is maximized, subject to the constraint on the energy capacity of the UAV. The problem dealt with in this paper poses great challenges due to: 1) it is difficult to model information redundancy of multiple photographs and 2) it is computationally expensive to find an energy-efficient flying tour for the UAV. To address the challenges, we will model the photograph quality by a submodular function. We will also propose a novel approximation algorithm with a provable approximation ratio within a quasi-polynomial time complexity, and a fast heuristic algorithm for the problem.

The main contributions of this paper are summarized as follows.

1) To the best of our knowledge, we are the first to consider a novel problem of finding an optimized flying tour for a UAV, such that the quality of photographs taken during the tour is maximized, subject to the limited energy capacity on the UAV.
2) We then propose a novel approximation algorithm with a quasi-polynomial time complexity. We also devise a fast yet scalable heuristic algorithm for the problem.
3) We finally evaluate the performance of the proposed algorithms via both a real and synthetic datasets through extensive simulations. Experimental results show that the proposed algorithms are very promising. Especially, the amounts of nonredundant information by the approximation and heuristic algorithms are about 11% and 8% more than that delivered by the state-of-the-art, respectively.

The remainder of this paper is organized as follows. We first introduce the system model, photograph quality model, and define the problem in Section II. We then propose a quasi-polynomial approximation algorithm and a fast yet scalable heuristic algorithm for the problem in Sections III and IV, respectively. We also evaluate the performance of the proposed algorithms in Section V. We finally review related work in Section VI, and conclude this paper in Section VII.

II. Preliminaries

In this section, we first introduce the network model, then propose a photograph quality model to characterize information redundancy of multiple photographs. We finally define the problem precisely, and show the NP-hardness of the problem.

A. Network Model

When a disaster (e.g., earthquakes, landslides, flooding, etc.) happens, people may not be able to approach to the disaster area very closely, due to risks and dangers in the area. To obtain the first-hand information about the disaster for rescue decision-making, we employ a UAV equipped with a camera to fly over the area, by taking photographs in the disaster area and sending the photographs back to an operation station via a wireless communication module built in the UAV (e.g., WiFi). For example, when an earthquake happens, we can dispatch a camera-equipped UAV located at a depot r initially to take photographs of destroyed buildings and injured people in that area.

We treat a disaster area as a 3-D space. Assume that there are m POIs $p_1, p_2, \ldots, p_m$ to be monitored in the area, where each POI p_j may be a school building, an office building, or a mall in the area, at which there are usually plenty of people. Let P be the set of these m POIs, i.e., $P = \{p_1, p_2, \ldots, p_m\}$.

It can be seen that there are infinite number of candidate positions that the UAV can hover and take photographs for POIs in a disaster area, this however makes the flying tour scheduling of the UAV intractable. For the sake of convenience, we here only consider a finite number of hovering positions in the area. We construct the candidate set V of hovering positions as follows. Initially, $V = \emptyset$. A position node v_i is added to V for each POI $p_i \in P$, where v_i is co-located with p_i. Furthermore, for the middle point v_i of any two POIs p_j and p_k in P, the position node v_i is added to V if the Euclidean distance between POIs p_j and p_k is no greater than a given length threshold τ (e.g., 50 m). The rationale behind this is that the UAV can take high resolution photographs for both POIs p_j and p_k simultaneously at their middle point v_i if p_j and p_k are close to each other [i.e., $d(p_j, p_k) \leq \tau$]. Otherwise ($d(p_j, p_k) > \tau$), the photographs taken at the middle point v_i may be with only low resolution for both p_j and p_k, and v_i thus is not an ideal hovering position for their monitoring. Then, it can be seen that $V = P \cup \{v_i | v_i$ is a middle point of two POIs p_j and p_k in P and $d(p_j, p_k) \leq \tau)\}$. Let $n = |V|$.

We use a complete graph $G = (\{r\} \cup V \cup P, E)$ with $d : E \mapsto \mathcal{R}^+$ to represent the potential tour network of the UAV, where $E = (\{r\} \cup V \cup P) \times (\{r\} \cup V \cup P)$ and d_{ij} is the Euclidean distance between any two nodes v_i and v_j in $\{r\} \cup V \cup P$.

We employ a UAV to take photographs for the m POIs ($m = |P|$). We assume that the UAV with an energy capacity B flies at a constant speed of ϑ (e.g., 10 m/s [25]). Since the energy consumption rate of the UAV for its operation (e.g., flying or hovering in the air) is very high, its battery energy can support its operation for only a limited duration T. For example, the operation duration of a fully charged DJI phantom 4 Pro UAV is about 30 min [25].

Since there are many POIs in a monitoring area, the UAV may not be able to visit each of the m POIs very closely, due to its limited energy capacity. Assume that the flying tour of the UAV is $C = r \to v_1 \to v_2 \to \cdots \to v_k \to r$, where r is the depot, v_i is a position in V at which the UAV can hover and take photographs for POIs, and k is a positive integer to be determined. Assume that the UAV hovers at each position v_i for δ time units to monitor nearby POIs (e.g., $\delta = 10$ s). Since the UAV is energy constrained, the accumulative time spent on its flying and taking photographs at hovering positions in tour C should be no greater than its longest operation duration T, due to its energy capacity, i.e., $[(\sum_{i=1}^{k+1} d(v_{i-1}, v_i))/\vartheta] + k\delta \leq T$, where $d(v_{i-1}, v_i)$ is the Euclidean distance between positions v_{i-1} and v_i and $v_0 = v_{k+1} = r$.

B. Photograph Quality Model

We note that a UAV can take photographs for multiple POIs at each hovering position v_i and each POI p_j can be monitored by the UAV at different hovering positions. Moreover, the quality of a photograph taken for a POI p_j at a hovering position v_i highly depends on the distance d_{ij} between them. That is, the shorter the distance, the higher the photograph quality. We thus define the quality $Q(I_{ij})$ of a photograph I_{ij} taken by the UAV at position v_i for a POI p_j as

$$Q(I_{ij}) = \frac{\xi}{d_{ij}} \tag{1}$$

where d_{ij} is the distance between position v_i and POI p_j and ξ is a given constant [15].

We then define the accumulative quality of all photographs taken at different hovering positions of a tour C for a single POI p_j. It can be seen that the more hovering positions that the UAV takes photographs for a specific POI, the more information about the POI can be obtained. Also, notice that the photographs for the same POI p_j at different hovering positions may be highly redundant. We thus make use of a submodular function $f(\cdot)$ to model the photograph quality for each POI p_j. This function characterizes the diminishing returns for monitoring POI p_j with more photographs taken at more hovering positions.

A function $f(\cdot) : 2^V \mapsto \mathcal{R}^+$ is a submodular function, if for any two sets $V_1, V_2 \subseteq V$ with $V_1 \subseteq V_2$, and any node $v \in V \backslash V_2$, such that $f(V_1 \cup \{v\}) - f(V_1) \geq f(V_2 \cup \{v\}) - f(V_2)$. Here, we use function $f(C, p_j)$ to quantify the amount of nonredundant information of photographs $I_{1j}, I_{2j}, \ldots, I_{kj}$ for a POI p_j taken at hovering positions $v_1, v_2, \ldots, v_k$ in tour C, e.g.,

$$f(C, p_j) = w_j \cdot \log_2 \left(\sum_{v_i \in C} Q(I_{ij}) + 1 \right) \tag{2}$$

where w_j is a given weight that indicates the importance of POI p_j (e.g., the weight w_j is large if there are many people at POI p_j).

The accumulative photograph quality $f(C, P)$ of tour C thus is the sum of photograph quality of all POIs at different hovering positions, i.e.,

$$f(C, P) = \sum_{p_j \in P} f(C, p_j). \tag{3}$$

C. Problem Definition

Although it is desirable to obtain accurate information for each POI for rescue decision-making, the energy budget of the UAV usually is unable to support its operation for a long time. In this paper we study the problem of employing a UAV to gather as much nonreductant information as possible, while the operation duration spent in the tour of the UAV is upper bounded by its longest operation duration T. Specially, given a complete graph $G = (\{r\} \cup V \cup P, E)$ with $d : E \mapsto \mathcal{R}^+$, a hovering duration δ at each hovering position, *the monitoring quality maximization problem* in G is to find a flying tour $C = r \to v_1 \to v_2 \to \cdots \to v_k \to r$ for the UAV such that the quality of photographs taken in its tour C is maximized, subject to that the total time spent by the UAV for flying and hovering in C is no greater than its longest operation duration T, i.e.,

$$\max f(C, P) \tag{4}$$

subject to

$$\frac{\sum_{i=1}^{k+1} d(v_{i-1}, v_i)}{\vartheta} + k\delta \leq T \tag{5}$$

where $v_0 = v_{k+1} = r$.

D. NP-Hardness of the Problem

We show that the monitoring quality maximization problem is NP-hard, by a polynomial time reduction from another NP-hard problem—the orienteering problem [4], which is defined as follows.

Given a complete graph $G' = (\{r\} \cup V', E')$, a length constraint T and a profit b_j associated with visiting each node $v'_j \in V'$, the orienteering problem is to find an r-rooted closed tour C in G' so that the sum of collected profits in C is maximized, subject to that the length of tour C is no greater than T [32].

Lemma 1: The monitoring quality maximization problem is NP-hard.

Proof: We reduce the orienteering problem to the monitoring quality maximization problem as follows. Consider the orienteering problem in a given undirected metric graph $G' = (\{r\} \cup V', E')$ with $d : E' \mapsto \mathcal{R}^+$ and a budget T. We construct an auxiliary graph $G = (\{r\} \cup V' \cup P, E)$ from G' by adding a virtual POI node p_j to P for each node v'_j in V'. We assume that the virtual node p_j is co-located with node v'_j. We assume that the UAV obtains the profit b_j for POI p_j if it visits v'_j, that is, $Q(I_{ij}) = b_j$ if $i = j$; otherwise ($i \neq j$), $Q(I_{ij}) = 0$. Thus, the orienteering problem in G' is a special case of the monitoring quality maximization problem G. Since the orienteering problem is NP-hard [8], the monitoring quality maximization problem is NP-hard, too. ■

E. Approximation Ratio

Given an optimization problem, denote by $\text{OPT}_{\mathcal{I}}$ the optimal value of an instance $\mathcal{I}$ of the problem. Also, denote by $\text{SOL}_{\mathcal{I}}$ the objective value of the solution delivered by an algorithm $\mathcal{A}$. For a maximization problem, the approximation ratio of algorithm $\mathcal{A}$ is R if $[(\text{SOL}_{\mathcal{I}})/(\text{OPT}_{\mathcal{I}})] \geq (1/R)$ for any problem instance $\mathcal{I}$, where $R \geq 1$. On the other hand, for a minimization problem, the approximation ratio of algorithm $\mathcal{A}$ is R if $[(\text{SOL}_{\mathcal{I}})/(\text{OPT}_{\mathcal{I}})] \leq R$ for any instance $\mathcal{I}$, where $R \geq 1$.

III. Quasi-Polynomial Approximation Algorithm

In this section, we propose an $O(\log n)$-approximation algorithm for the monitoring quality maximization problem, which is to find a flying tour C for a UAV with its total flying duration being no greater than a given value T, such that the accumulative quality of photographs taken in C is maximized.

The basic idea behind the proposed algorithm is to reduce the problem to another submodular orienteering problem (SOP), through a series of novel graph transformations, where the transformations will be shown in Sections III-A and III-B later, and an approximate solution to the SOP in turn returns an approximate solution to the original problem.

The SOP [4] is defined as follows. Given a complete graph $G' = (V', E')$ with $d' : E' \mapsto \mathcal{Z}^+$, a start node s and an end node t in V', and a submodular reward function $f' : 2^{V'} \mapsto \mathcal{Z}^+$, the edge weights in G' satisfy the triangle inequality. The problem is to find a path C in G' from s to t, such that the collected reward $f'(C)$ in C is maximized, while ensuring that the length of C is no greater than a given length bound T.

A. Transforming the Original Graph G to Another Equivalent Graph G_1

Notice that the original graph G is both edge-weighted and node-weighted, which makes the monitoring quality maximization problem difficult to be solved. We transform G to another only edge-weighted graph G_1, and we show that the problem in G is equivalent to the problem in G_1. A solution to the problem in G_1 then returns a solution to the problem in G.

Given a complete graph $G = (\{r\} \cup V \cup P, E)$ with $d : E \mapsto \mathcal{R}^+$, a hovering duration δ at each hovering position in V, a longest flying duration T and a submodular function $f(C, P) = \sum_{p_j \in P} f(C, p_j)$, an auxiliary graph $G_1 = (V_1, E_1)$ with $d_1 : E_1 \mapsto \mathcal{R}^+$ and $f_1 : 2^{V_1} \mapsto \mathcal{R}^+$ is constructed from G as follows. Two virtual nodes s and t for the depot r are added to V_1, and both nodes s and t are co-located with r. Let $V_1 = V \cup \{s, t\}$ and $E_1 = V_1 \times V_1$. For any two nodes u and v in V_1, the weight $d_1(u, v)$ of edge (u, v) in E_1 is

$$d_1(u, v) = \frac{d(u, v)}{\vartheta} + \frac{\Delta(u) + \Delta(v)}{2} \tag{6}$$

where $d(u, v)$ is the Euclidean distance between nodes u and v, ϑ is the flying speed of the UAV, $\Delta(u)$ and $\Delta(v)$ are the hovering durations of the UAV at nodes u and v, respectively. Specifically, $\Delta(v) = \delta$ if $v \neq s$ and $v \neq t$ for any node v in V_1; otherwise ($v = s$ or $v = t$), $\Delta(v) = 0$. Also, let $f_1(C) = \sum_{p_j \in P} f(C, p_j)$.

We illustrate the graph transformation from G to G_1 via an example, see Fig. 2(a) and (b). For example, the weight $d_1(v_1, v_2)$ of edge (v_1, v_2) in G_1 is $d_1(v_1, v_2) = [(d(v_1, v_2))/\vartheta] + [(\Delta(v_1) + \Delta(v_2))/2] = (228 \text{ m}/10 \text{ m/s}) + (10 \text{ s} + 10 \text{ s}/2) = 32.8$ s, where $d(v_1, v_2)$ is the Euclidean distance between v_1 and v_2 in G.

We claim that the monitoring quality maximization problem in G is equivalent to the problem of finding an $s-t$ path C in G_1 such that the value of $f_1(C)$ is maximized, while ensuring that the length of path C is no greater than T. We will show the claim later.

B. Transforming Graph G_1 to Another Auxiliary Graph G_2

To apply the quasi-polynomial approximation algorithm in [4] for the SOP, it must meet two prerequisites: 1) both the values of reward $f'(V'_s)$ of any subset V'_s of V' and edge weights are positive integers and 2) the value of an optimal solution is polynomially bounded by the number of nodes in V'. However, the reward values and edge weight values in G_1 may not be integers, and the value OPT_1 of an optimal solution to the problem in G_1 may not be polynomially bounded by the number of nodes in V_1.

We transform G_1 into another auxiliary graph G_2, such that graph G_2 satisfies the two prerequisites of applying the approximation algorithm in [4], through the use of the scaling and rounding techniques. We then solve the SOP problem in G_2 by applying the algorithm in [4]. We also show that an approximate solution to the problem in G_2 returns to an approximate solution to the problem in G_1 with a loss of the approximation ratio at most ϵ, where ϵ is a given constant such that $(1/\epsilon)$ is a positive integer $0 < \epsilon \leq 1$, i.e., $\epsilon = 1, (1/2), (1/3), (1/4), \ldots$

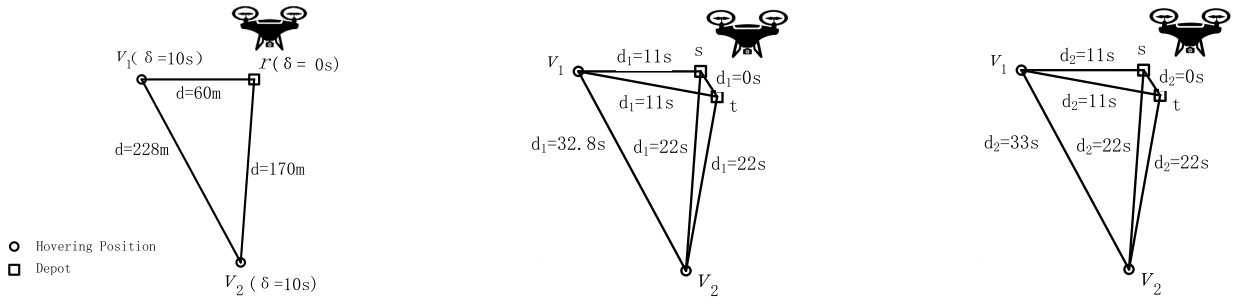

Fig. 2. Graph transformations from G to G_1 and from G_1 to G_2, where a UAV will fly at a speed $\vartheta = 10$ m/s and hover at each node for $\delta = 10$ s. Set $\tau_0 = 1$ s when transforming graph G_1 to G_2. (a) $G = (\{r \cup V \cup P, E)$ with $d : E \mapsto \mathcal{R}^+$. (b) $G_1 = (V_1, E_1)$ with $d_1 : E_1 \mapsto \mathcal{R}^+$. (c) $G_2 = (V_2, E_2)$ with $d_2 : E_2 \mapsto \mathcal{Z}^+$.

Given a graph $G_1 = (V_1, E_1)$ with $d_1 : E_1 \mapsto \mathcal{R}^+$ and $f_1 : 2^{V_1} \mapsto \mathcal{R}^+$, we show the graph transformation from G_1 to $G_2 = (V_2, E_2)$ with $d_2 : E_2 \mapsto \mathcal{Z}^+$ and $f_2 : 2^{V_2} \mapsto \mathcal{Z}^+$ as follows. G_2 has the identical topological structure as G_1, i.e., $V_2 = V_1$ and $E_2 = E_1$. Denote by $f_{\max}$ the maximum quality of photographs taken at any hovering position v in V_1, i.e., $f_{\max} = \max_{v \in V_1}\{f_1(v)\}$. Let $\varphi = \epsilon \cdot f_{\max}$ be a scaling factor, where ϵ is a given constant with $0 < \epsilon \leq 1$ such that $(1/\epsilon)$ is a positive integer. We set $f_2(V_s) = \lfloor (f_1(V_s)/\varphi) \rfloor$ for each subset $V_s \subseteq V_1$. On the other hand, given a small time unit τ_0 (e.g., τ_0=1 s), let $d_2(u, v) = \lceil (d_1(u, v)/\tau_0) \rceil$ for any edge (u, v) in E_2 and $T_2 = \lfloor (T/\tau_0) \rfloor$. We use an example to illustrate the transformation from G_1 to G_2, see Fig. 2(b) and (c). For example, the edge weight $d_2(v_1, v_2)$ in G_2 is $d_2(v_1, v_2) = \lceil (d_1(v_1, v_2)/\tau_0) \rceil = \lceil (32.8 \text{ s}/1) \rceil = 33$ s when $\tau_0 = 1$ s.

It can be seen that graph G_2 meets the prerequisite: 1) that both the values $f_2(V_s)$ and its edge weights are positive integers, and we later will show that the optimal value OPT_2 of the SOP in G_2 satisfies the prerequisite and 2) that OPT_2 is polynomially bounded by the number of nodes in V_2, i.e., there is a constant $c > 0$ such that $\text{OPT}_2 = O(n_2^c)$, where $n_2 = |V_2|$.

Having graph G_2, an $O(\log \text{OPT}_2)$-approximate solution to the SOP in it is then obtained, by applying the algorithm due to Chekuri and Pál [4], and the solution will be shown an $O(\log n)$-approximate solution to the monitoring quality maximization problem in the original graph G. The detailed algorithm is presented in `Algorithm 1`.

C. Algorithm Analysis

In the following, we analyze the performance of the proposed algorithm, `Algorithm 1`. We first show that the optimal value of the monitoring quality maximization problem in G is equal to that in G_1 by Lemma 2. We then prove that the optimal value of the SOP in G_2 is polynomially bounded by Lemma 3. Therefore, we can apply the quasi-polynomial approximation algorithm in [4] for the SOP in G_2, and an R-approximate solution then can be delivered with $R \geq 1$. We further show that an R-approximate solution to the SOP in G_2 returns to an $(R + \epsilon)$-approximate solution to the monitoring quality maximization problem in G_1 by Lemma 4. We finally show that `Algorithm 1` delivers an $O(\log n)$-approximate solution by Theorem 1.

Algorithm 1 `ApproAlg`

Input: A complete graph $G = (\{r\} \cup V \cup P, E)$ with $d : E \mapsto \mathcal{R}^+$, a given time budget T, a hovering duration δ at each node in V, a given flying speed ϑ of the UAV and a submodular function $f(C, P) = \sum_{p_j \in P} f(C, p_j)$.

Output: A closed tour C such that the total quality of photographs $f(C, P)$ taken in tour C is maximized, while the consumed time in C is no greater than T.

1: Transform graph G to another auxiliary graph $G_1 = (V_1, E_1)$ with $d_1 : E_1 \mapsto \mathcal{R}^+$ and $f_1 : 2^{V_1} \mapsto \mathcal{R}^+$, where virtual nodes s and t are co-located with r, $V_1 = V \cup \{s, t\}$, $E_1 = V_1 \times V_1$, $d_1(u, v) = \frac{d(u,v)}{\vartheta} + \frac{\Delta(u)+\Delta(v)}{2}$ for each edge (u, v) in E_2, and $f_1(C) = f(C, P)$;

2: Transform graph G_1 to another auxiliary graph $G_2 = (V_2, E_2)$ with $d_2 : E_2 \to \mathcal{Z}^+$ and $f_2 : 2^{V_2} \mapsto \mathcal{Z}^+$, where $V_2 = V_1$, $E_2 = E_1$, $f_2(V_s) = \lfloor \frac{f_1(V_s)}{\varphi} \rfloor$ for any subset $V_s \subseteq V_1$, $\varphi = \epsilon \cdot f_{max}$ with $0 < \epsilon \leq 1$ and $\frac{1}{\epsilon}$ is a positive integer, $f_{max} = \max_{v \in V_1}\{f_1(v)\}$, $d_2 = \lceil \frac{d_1}{\tau_0} \rceil$ and $T_2 = \lfloor \frac{T}{\tau_0} \rfloor$;

3: Find a path C in G_2 from s to t such that the total quality of photographs $f_2(C)$ taken in C is maximized, while the consumed time in C is no greater than T_2, by applying the approximation algorithm for the SOP due to Chekuri and Pál [4];

4: **return** tour C.

Lemma 2: Given a complete graph $G = (\{r\} \cup V \cup P, E)$ with $d : E \mapsto \mathcal{R}^+$, a submodular function $f(C, P)$, a hovering duration δ at each node in V and flying speed ϑ of the UAV, an auxiliary graph $G_1 = (V_1, E_1)$ with $d_1 : E_1 \mapsto \mathcal{R}^+$ and $f_1 : 2^{V_1} \mapsto \mathcal{R}^+$ is constructed from G, where $d_1(u, v) = (d(u, v)/\vartheta) + [(\Delta(u) + \Delta(v))/2]$ and $f_1(C) = f(C, P)$. Then, the optimal value of the monitoring quality maximization problem in G is equal to the optimal value of the problem in G_1.

Proof: Let C^* and C_1^* be the optimal solutions to the monitoring quality maximization problem in G and G_1, and OPT and OPT_1 be the values of C^* and C_1^*, respectively, where $C^* = r \to u_1^* \to u_2^* \to \cdots \to u_k^* \to r$ and $C_1^* = s \to v_1^* \to v_2^* \to \cdots \to v_{k_1}^* \to t$. In the following, we show $\text{OPT} = \text{OPT}_1$ by proving $\text{OPT} \leq \text{OPT}_1$ and $\text{OPT}_1 \leq \text{OPT}$.

We first show that $\text{OPT} \leq \text{OPT}_1$. Given an optimal solution $C^* = r \to u_1^* \to u_2^* \to \cdots \to u_k^* \to r$ to the problem in G, then $\text{OPT} = f(C^*)$ and the time duration $d(C^*)$ of tour C^* is no greater than T, i.e., $d(C^*) \leq T$. We now show that path $C = s \to u_1^* \to u_2^* \to \cdots \to u_k^* \to t$ is a feasible solution to

the problem in G_1, since

$$\begin{aligned} d_1(C) &= d_1\big(s, u_1^*\big) + \sum_{i=1}^{k-1} d_1\big(u_i^*, u_{i+1}^*\big) + d_1\big(u_k^*, t\big) \\ &= \frac{d\big(s, u_1^*\big)}{\vartheta} + \frac{\delta}{2} + \sum_{i=1}^{k-1}\left(\frac{d\big(u_i^*, u_{i+1}^*\big)}{\vartheta} + \frac{\delta+\delta}{2}\right) \\ &\quad + \frac{d\big(u_k^*, t\big)}{\vartheta} + \frac{\delta}{2}, \text{by (6)} \\ &= \frac{d\big(r, u_1^*\big)}{\vartheta} + \sum_{i=1}^{k-1} \frac{d\big(u_i^*, u_{i+1}^*\big)}{\vartheta} + \frac{d\big(u_k^*, r\big)}{\vartheta} + k \cdot \delta \\ &= d\big(C^*\big) \le T. \end{aligned} \tag{7}$$

We thus have $f_1(C) = f(C^*) = \text{OPT}$ and $f_1(C) \le f_1(C_1^*) = \text{OPT}_1$ as C_1^* is an optimal solution to the problem in G_1, i.e., $\text{OPT} \le \text{OPT}_1$.

We then show that $\text{OPT}_1 \le \text{OPT}$. Given an optimal solution $C_1^* = s \to v_1^* \to v_2^* \to \cdots \to v_{k_1}^* \to t$ for the problem in G_1. We know that $\text{OPT}_1 = f_1(C_1^*)$ and the time duration $d_1(C_1^*)$ of tour C_1^* is no greater than T. We show that tour $C_1 = r \to v_1^* \to v_2^* \to \cdots \to v_{k_1}^* \to r$ is a feasible solution to the problem in G, because

$$\begin{aligned} d(C_1) &= \frac{d\big(r, v_1^*\big)}{\vartheta} + \sum_{i=1}^{k_1-1} \frac{d\big(v_i^*, v_{i+1}^*\big)}{\vartheta} + \frac{d\Big(v_{k_1}^*, r\Big)}{\vartheta} + k_1 \cdot \delta \\ &= \frac{d\big(r, v_1^*\big)}{\vartheta} + \frac{\delta}{2} + \sum_{i=1}^{k_1-1}\left(\frac{d\big(v_i^*, v_{i+1}^*\big)}{\vartheta} + \frac{\delta+\delta}{2}\right) \\ &\quad + \frac{d\Big(v_{k_1}^*, r\Big)}{\vartheta} + \frac{\delta}{2} \\ &= \frac{d_1\big(s, v_1^*\big)}{\vartheta} + \sum_{i=1}^{k_1-1} \frac{d_1\big(v_i^*, v_{i+1}^*\big)}{\vartheta} + \frac{d_(v_{k_1}^*, t)}{\vartheta}, \text{by (6)} \\ &= d_1\big(C_1^*\big) \le T. \end{aligned} \tag{8}$$

We thus conclude that $f(C_1) = f_1(C_1^*) = \text{OPT}_1$ and $f(C_1) \le f(C^*) = \text{OPT}$ as C^* is an optimal solution to the problem in G, i.e., $\text{OPT}_1 \le \text{OPT}$. The lemma then follows. ■

We then show that the optimal value in graph G_2 is polynomially bounded by the following lemma.

Lemma 3: Given a complete graph $G_1 = (V_1, E_1)$ with $d_1 : E_1 \mapsto \mathcal{R}^+$ and $f_1 : 2^{V_1} \mapsto \mathcal{R}^+$, transform graph G_1 to $G_2 = (V_2, E_2)$ with $d_2 : E_2 \to \mathcal{Z}^+$ and $f_2 : 2^{V_2} \mapsto \mathcal{Z}^+$, where $V_2 = V_1$, $E_2 = E_2$, $f_2(V_s) = \lfloor (f_1(V_s)/\varphi) \rfloor$ of any subset $V_s \subseteq V_1$, $\varphi = \epsilon \cdot f_{\max}$ with $0 < \epsilon \le 1$ and $(1/\epsilon)$ is a positive integer, $f_{\max} = \max_{v \in V_1}\{f_1(v)\}$, and $d_2 = \lceil (d_1/\lambda) \rceil$, the optimal value OPT_2 of the SOP in G_2 is between $(1/\epsilon)$ and (n/ϵ), i.e., $(1/\epsilon) \le \text{OPT}_2 \le (n/\epsilon)$.

Proof: Let C_2^* be an optimal solution to the problem in G_2, i.e., $\text{OPT}_2 = f_2(C_2^*)$. We show that $(1/\epsilon) \le \text{OPT}_2 \le (n/\epsilon)$, where ϵ a given constant with $0 < \epsilon \le 1$ such that $(1/\epsilon)$ is an positive integer. We first show that $\text{OPT}_2 \ge (1/\epsilon)$, since

$$\begin{aligned} \text{OPT}_2 &= f_2\big(C_2^*\big) \\ &= \left\lfloor \frac{f_1\big(C_2^*\big)}{\varphi} \right\rfloor, \text{ by the definition of } f_2\big(C_2^*\big) \\ &= \left\lfloor \frac{f_1\big(C_2^*\big)}{\epsilon \cdot f_{\max}} \right\rfloor, \text{ as } \varphi = \epsilon \cdot f_{\max} \\ &\ge \left\lfloor \frac{f_{\max}}{\epsilon \cdot f_{\max}} \right\rfloor, \text{ as } f_1\big(C_2^*\big) \ge \max_{v \in V_1}\{f_1(v)\} = f_{\max} \\ &= \frac{1}{\epsilon}, \text{ as } \frac{1}{\epsilon} \text{ is a positive integer.} \end{aligned} \tag{9}$$

We then prove that $\text{OPT}_2 \le (n/\epsilon)$. Let $V_2 = \{v_1, v_2, \ldots, v_n, s, t\}$ and $V_2' = V_2 \backslash \{s, t\}$, i.e., $V_2' = \{v_1, v_2, \ldots, v_n\}$. We have

$$\begin{aligned} \text{OPT}_2 &= f_2\big(C_2^*\big) \\ &\le f_2(V_2), \text{as the set of nodes in } C_2^* \text{ is a subset of } V_2 \\ &= f_2\big(V_2'\big), \text{ as } f_2(\{s, t\}) = 0 \\ &= f_2\big(V_2'\big) - f_2\big(V_2' \backslash \{v_1\}\big) + f_2\big(V_2' \backslash \{v_1\}\big) \\ &\le f_2(v_1) - f_2(\emptyset) + f_2\big(V_2' \backslash \{v_1\}\big) \\ &\quad \text{by the sub modularity of } f_2 \text{ and } \emptyset \subseteq V_2' \backslash \{v_1\} \\ &= f_2(v_1) + f_2\big(V_2' \backslash \{v_1\}\big), \text{ as } f_2(\emptyset) = 0 \\ &\le f_2(v_1) + f_2(v_2) + f_2\big(V_2' \backslash \{v_1, v_2\}\big) \\ &\quad \vdots \\ &\le \sum_{i=1}^{n} f_2(v_i) \\ &= \sum_{i=1}^{n} \left\lfloor \frac{f_1(v_i)}{\epsilon \cdot f_{\max}} \right\rfloor, \text{ by the definition of } f_2(v_i) \\ &\le \sum_{i=1}^{n} \left\lfloor \frac{f_{\max}}{\epsilon \cdot f_{\max}} \right\rfloor, \quad \text{as } f_1(v_i) \le \max_{v_i \in V_2'}\{f(v_i)\} = f_{\max} \\ &= \frac{n}{\epsilon}. \end{aligned} \tag{10}$$

Combining Inequalities (9) and (10), it can be seen that the optimal value OPT_2 of the problem in G_2 is between $(1/\epsilon)$ and (n/ϵ), i.e., $(1/\epsilon) \le \text{OPT}_2 \le (n/\epsilon)$. ■

We further prove that an R-approximate solution to the problem in G_2 returns to an $(R+\epsilon)$-approximate solution to the problem in G_1, by the following lemma.

Lemma 4: An R-approximate solution to the problem in G_2 returns to an $(R+\epsilon)$-approximate solution to the problem in G_1 with $R \ge 1$.

Proof: Let C_1^* and C_2^* be the optimal solutions to the SOP in G_1 and G_2, respectively. Let C_2 be an R-approximate solution to the SOP in G_2 delivered by an approximation algorithm with $R \ge 1$. It can be easily shown that C_2 is a feasible solution in G_1 with a similar proof as that in Lemma 3, omitted. In the following, we only analyze the ratio of the solution C_2 to the optimal solution C_2^*.

Since C_2 is an R-approximate solution in G_2, the ratio of the accumulative quality of photographs taken in the optimal solution C_2^* to the total quality of photographs taken in tour C_2 is no greater than R, i.e., $[(f_2(C_2^*))/(f_2(C_2))] \le R$. We now

bound the approximation ratio of solution C_2, i.e., the ratio of $f_1(C_1^*)$ to $f_1(C_2)$.

On one hand, the accumulative quality of photographs taken in the optimal solution C_1^* to the problem in graph G_1 is

$$\begin{aligned} f_1(C_1^*) &= \frac{f_1(C_1^*)}{\epsilon}\cdot\epsilon \\ &\le \left(\left\lfloor\frac{f_1(C_1^*)}{\epsilon}\right\rfloor+1\right)\cdot\epsilon \\ &= \left(f_2(C_1^*)+1\right)\cdot\epsilon, \text{ since } f_2(C_1^*)=\left\lfloor\frac{f_1(C_1^*)}{\epsilon}\right\rfloor \\ &\le \left(f_2(C_2^*)+1\right)\cdot\epsilon \\ &\quad \text{as } C_2^* \text{ is an optimal solution in } G_2, \\ &\le (R\cdot f_2(C_2)+1)\cdot\epsilon, \\ &\quad \text{as } f_2(C_2^*)\le R\cdot f_2(C_2). \end{aligned} \tag{11}$$

On the other hand, the total quality of photographs taken in tour C_2 is

$$\begin{aligned} f_1(C_2) &= \frac{f_1(C_2)}{\epsilon}\cdot\epsilon \\ &\ge \left\lfloor\frac{f_1(C_2)}{\epsilon}\right\rfloor\cdot\epsilon \\ &= f_2(C_2)\cdot\epsilon, \text{ since } f_2(C_2)=\left\lfloor\frac{f_1(C_2)}{\epsilon}\right\rfloor. \end{aligned} \tag{12}$$

Then, the approximation ratio of `Algorithm 1` for tour C_2 in G_1 is

$$\begin{aligned} \frac{f_1(C_1^*)}{f_1(C_2)} &\le \frac{(R\cdot f_2(C_2)+1)\cdot\epsilon}{f_2(C_2)\cdot\epsilon} \\ &= R+\frac{1}{f_2(C_2)} \\ &\le R+\epsilon, \text{ as } f_2(C_2)\ge\frac{1}{\epsilon} \text{ by Lemma 3.} \end{aligned} \tag{13}$$

■

We thus have the following theorem.

Theorem 1: Given a complete graph $G=(\{r\}\cup V\cup P,E)$ with $d: E\mapsto\mathcal{R}^+$) and a submodular function $f(C,P)$, a hovering duration δ at each node in V except the depot r, and a flying speed ϑ of the UAV, there is a quasi-polynomial $O(\log n)$-approximation algorithm, `Algorithm 1`, for the monitoring quality maximization problem with time complexity of $O(m(n\cdot\log T)^{O(\log n)})$, where $n=|V|$, $m=|P|$, and T is the longest operation duration of the UAV.

Proof: Following Lemma 2, the optimal value OPT of the monitoring quality maximization problem in G is equal to the optimal value OPT_1 of the problem in G_1, i.e., $\mathrm{OPT}=\mathrm{OPT}_1$. At the same time, an R-approximate solution to the problem in G_2 returns to an $(R+\epsilon)$-approximate solution to the problem in G_1 by Lemma 4.

On the other hand, the algorithm in [4] finds an $O(\log \mathrm{OPT}_2)$-approximate solution C_2 in G_2 in time $O(m(n\cdot\log T)^{O(\log n)})$, where OPT_2 is the optimal value of the SOP in G_2. The approximation ratio of the optimal value OPT to the value of the approximate solution C_2 delivered by `Algorithm 1` in the original graph G then is

$$\begin{aligned} \frac{\mathrm{OPT}}{f(C_2)} &= \frac{\mathrm{OPT}_1}{f_1(C_2)}, \text{ as } \mathrm{OPT}=\mathrm{OPT}_1, f(C_2)=f_1(C_2) \\ &\le R+\epsilon, \text{ by Lemma 4} \\ &= O(\log \mathrm{OPT}_2), \text{ where } R=O(\log \mathrm{OPT}_2) \\ &\quad \text{and } \epsilon \text{ is a constant} \\ &= O(\log n), \text{ as } \mathrm{OPT}_2\le\frac{n}{\epsilon} \text{ by Lemma 3} \\ &\quad \text{and } \frac{1}{\epsilon} \text{ is a constant.} \end{aligned} \tag{14}$$

The time complexity analysis is followed by Chekuri and Pál [4], omitted. ■

IV. Fast Heuristic Algorithm

In the previous section, we proposed a quasi-polynomial approximation algorithm with running time $O(m(n\cdot\log T)^{O(\log n)})$ for the monitoring quality maximization problem, where m and n are the numbers of POIs and hovering positions, respectively, and T is the longest flying duration of the UAV. However, its running time is prohibitively high for a large-scale monitoring area, e.g., there are tens of thousands of POIs in a disaster area. In this section, we devise a fast yet scalable heuristic algorithm for the problem.

The basic idea behind the heuristic lies in an important observation. That is, any tree $\mathcal{T}$ can be transformed into a closed tour C with the cost of C being no more than twice the cost of tree $\mathcal{T}$. Thus, we can incrementally expand the tree $\mathcal{T}$, such that the cost of its transformed tour C is no greater than a given time bound T and the quality of photographs taken in C is maximized.

In the following, we first introduce a technique that transforms a tree to a closed tour, then describe the heuristic algorithm, finally analyze its time complexity.

For a weighted graph $G_1=(V_1,E_1)$ with a cost function $d_1: E_1\mapsto\mathcal{R}^+$, denote by $d_1(G_1)$ *the cost* of G_1, which is the weighted sum of edges in E_1, i.e., $d_1(G_1)=\sum_{(u,v)\in E_1} d_1(u,v)$.

Given a tree $\mathcal{T}$ with cost $d_1(\mathcal{T})$, we introduce a technique that transforms tree $\mathcal{T}$ to a closed tour C [33]. An Eulerian graph G_e is obtained by duplicating each edge in tree $\mathcal{T}$. It is obvious that the cost of the Eulerian graph G_e is $2\cdot d_1(\mathcal{T})$. An Eulerian circuit C_e then can be derived, where C_e visits each edge in G_e once and once only, as the degree of each node in G_e is even. A simple closed tour C can be obtained ultimately, by shortcutting duplicated nodes in circuit G_e. The cost $d_1(C)$ of tour C is no greater than the cost of Eulerian circuit $d_1(C_e)$ due to the triangle inequality. Therefore, $d_1(C)\le d_1(C_e)=d_1(G_e)=2\cdot d_1(\mathcal{T})$.

Lemma 5: Given a tree $\mathcal{T}$ with cost $d_1(\mathcal{T})$, the cost $d_1(C)$ of the tour C transformed from tree $\mathcal{T}$ is no more than twice the cost of $\mathcal{T}$, i.e., $d_1(C)\le 2\cdot d_1(\mathcal{T})$ [33].

A. Algorithm

Given a complete graph $G=(\{r\}\cup V\cup P,E)$ with $d: E\mapsto\mathcal{R}^+$, a hovering duration δ at each node in V, a

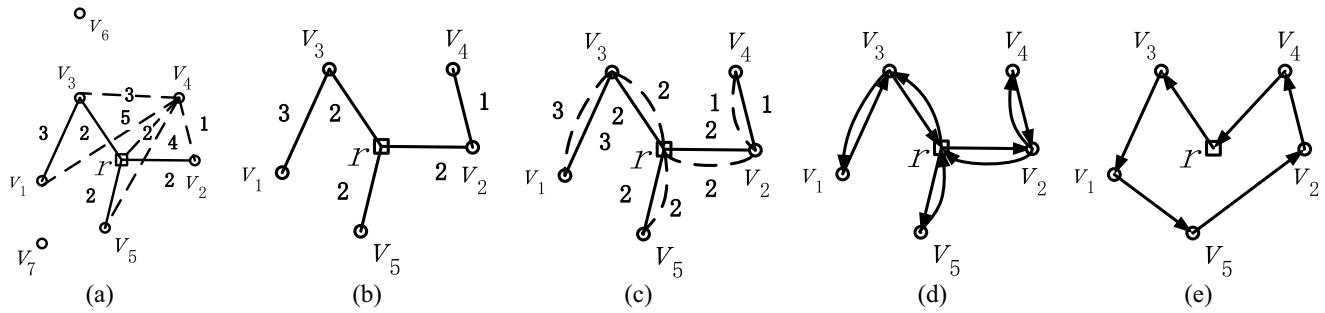

Fig. 3. Procedure of obtaining a new tree. (a) A r-rooted tree $\mathcal{T}$ spanning nodes r, v_1, v_2, v_3, v_5. (b) Construct a new tree $\mathcal{T}_4$ by connecting v_4 to its nearest node v_2 in $\mathcal{T}$. (c) An Eulerian graph G_{e_4} is derived by duplicating each edge in $\mathcal{T}_4$. (d) An Eulerian circuit $C_{e_4} = r \to v_3 \to v_1 \to v_3 \to r \to v_5 \to r \to v_2 \to v_4 \to v_2 \to r$ in graph G_{e_4} is obtained. (e) A closed tour $C_4 = r \to v_3 \to v_1 \to v_5 \to v_2 \to v_4 \to r$ is derived by shortcutting duplicated nodes in C_{e_4}.

flying speed ϑ, a longest operation duration T, and a submodular function $f(C, P) = \sum_{p_j \in P} f(C, p_j)$, we first transform graph G to another equivalent graph G_1, then find a tree $\mathcal{T}$ in G_1 and transform the tree to a closed tour C, such that the total quality of photographs in tour C is maximized, subject to that the cost of $d_1(C)$ is no greater than T.

Graph G is first transformed to another equivalent graph $G_1 = (V_1, E_1)$ with $d_1 : E_1 \mapsto \mathcal{R}^+$ and $f_1 : 2^{V_1} \mapsto \mathcal{R}^+$, where $V_1 = \{r\} \cup V$, $E_1 = V_1 \times V_1$, $d_1 = (d(u, v)/\vartheta) + [(\Delta(u) + \Delta(v))/2]$, $f_1(C) = f(C, P)$. Specifically, $\Delta(v) = \delta$ if $v \neq r$ for any node $v \in V_1$; otherwise ($v = r$), $\Delta(v) = 0$. It can be seen that the optimal value of the monitoring maximization problem in G is equal to the optimal value of the problem in G_1, and its proof follows by Lemma 2, omitted.

The heuristic algorithm constructs a tree $\mathcal{T} = (V_t, E_t)$ in G_1 iteratively. Tree $\mathcal{T}$ consists of a single node, deport r, initially, i.e., tree $\mathcal{T} = (V_t = \{r\}, E_t = \emptyset)$. Assume that part of tree $\mathcal{T} = (V_t, E_t)$ with $V_t \subseteq \{r\} \cup V_1$ has been constructed, and the cost $d_1(C)$ of the closed tour C transformed from tree $\mathcal{T}$ is no greater than T. We now expand tree $\mathcal{T}$ by adding a new node $v \in V_1 \backslash V_t$ to it. For each candidate v_i in $V_1 \backslash V_t$, we can obtain a new tree $\mathcal{T}_i$ by connecting v_i to its nearest node in tree $\mathcal{T}$. We then deliver a closed tour C_i transformed from $\mathcal{T}_i$.

We illustrate the procedure of obtaining a new tree $\mathcal{T}_i$ and transforming $\mathcal{T}_i$ to a closed tour C_i via an example, see Fig. 3. For example, we have a tree $\mathcal{T}$ spanning nodes r, v_1, v_2, v_3, and v_5. We now consider adding v_4 to $\mathcal{T}$, see Fig. 3(a). The nearest node in $\mathcal{T}$ of v_4 is node v_2 with cost $d_1(v_4, v_2) = 1$. Fig. 3(b) shows the tree $\mathcal{T}_4$ by adding v_4 to $\mathcal{T}$. An Eulerian graph G_{e_4} then is obtained by duplicating each edge in $\mathcal{T}_4$, see Fig. 3(c), and an Eulerian circuit C_{e_4} then is obtained from the Eulerian graph, see Fig. 3(d). A closed tour C_4 finally is derived from the Eulerian circuit, by shortcutting duplicated nodes in C_{e_4}, see Fig. 3(e).

If the cost $d_1(C_i)$ of tour C_i is strictly larger than T, i.e., $d_1(C_i) > T$, v_i cannot be added to tree $\mathcal{T}$. Consider the subset $V' \subseteq V_1 \backslash V_t$ that each node v_i in V' can be added to tree $\mathcal{T}$, i.e., $V' = \{v_i | v_i \in V_1 \backslash V_t, d_1(C_i) \leq T\}$, we calculate the marginal gain $g(v_i)$ by adding node v_i to $\mathcal{T}$, which is given as follows:

$$g(v_i) = f_1(V_t \cup v_i) - f_1(V_t). \tag{15}$$

Algorithm 2 `TreeAlg`

Input: A graph $G = (\{r\} \cup V \cup P, E)$ with $d : E \mapsto \mathcal{R}^+$, a given time budget T, a hovering duration δ at each node in V, and a flying speed ϑ of the UAV

Output: A closed tour C such that the total quality $f(C, P)$ of photographs taken in tour C is maximized, while the consumed time in C is no greater than T.

```
Transform graph G into another equivalent graph G_1 = (V_1, E_1) with d_1 : E_1 ↦ R^+ and f_1 : 2^{V_1} ↦ R^+, where V_1 = {r} ∪ V, E_1 = V_1 × V_1, d_1(u,v) = d(u,v)/ϑ + (Δ(u)+Δ(v))/2 for each edge (u,v) in E_1, f_1(C) = f(C,P);
Let T = ({r}, ∅), i.e., V_t = {r}, d_1(C) = 0;
while V_t ≠ V_1 and d_1(C) ≤ T do
    V' ← ∅;
    for each v_i ∈ V_1\V_t do
        Construct a new tree T_i by connecting node v_i to its nearest node in T, and obtain a closed tour C_i transformed from T_i;
        if d_1(C_i) ≤ T then
            V' ← V' ∪ {v_i};
        end if
    end for
    for each v_i ∈ V' do
        Calculate the marginal gain g(v_i) by Eq. (15);
    end for
    Choose a node v_j with the maximum ratio of its marginal gain g(v_j) to its increased cost d_1(C_j) − d_1(C) by Eq. (16), and add v_j to the tree T;
    Obtain a closed tour C transformed from the new tree T;
end while
return tour C.
```

A node v_j with the maximum ratio of its marginal gain to its increased cost from $d_1(C)$ to $d_1(C_j)$ is then chosen, i.e.,

$$v_j = \arg\max_{v_i \in V'} \frac{f_1(V_t \cup v_i) - f_1(V_t)}{d_1(C_i) - d_1(C)}. \tag{16}$$

This process continues until either all nodes in V_1 have been added to $\mathcal{T}$ or the addition of any node in $V_1 \backslash V_t$ to $\mathcal{T}$ will violate the cost upper bound T.

The detailed algorithm for the monitoring quality maximization problem is described in `Algorithm 2`.

Theorem 2: Given a complete graph $G = (\{r\} \cup V \cup P, E)$ with $d : E \mapsto \mathcal{R}^+$, there is a heuristic algorithm, `Algorithm 2`, for the monitoring quality maximization

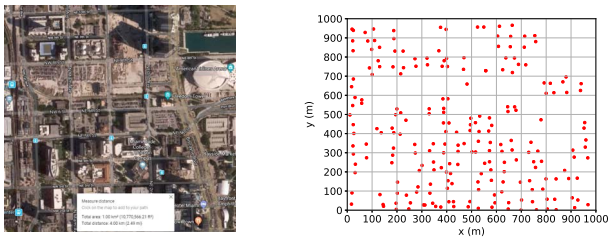

(a) (b)

Fig. 4. Monitoring area and the locations of POIs. (a) Network in a $1000 \times 1000 \times 500$ m^3 3-D area at Miami county, USA. (b) $(x,\ y)$ coordinates of the $m = 223$ POIs in the network.

problem in G with time complexity $O(n^3 + n^2 m)$, where $n = |V|$ and $m = |P|$.

Proof: The time complexity analysis is straightforward, omitted. ■

V. Performance Evaluation

In this section, we evaluate the performance of the proposed algorithms. We also study the impact of important parameters on the performance of the proposed algorithms.

A. Experimental Settings

We consider both a real network and synthetic networks. Specifically, we consider a real network in a $1000 \times 1000 \times 500$ m^3 3-D disaster area at Miami county, USA, where the hurricane Irma struck it on September 14, 2017, see Fig. 4(a). There are $m = 223$ POIs in the area, where each POI is a building, school, church, or government office, etc., see Fig. 4(b). On the other hand, for synthetic networks, we assume that each network is also in a $1000 \times 1000 \times 500$ m^3 3-D space. There are from 50 to 200 POIs in the network, where the location $(x,\ y,\ z)$ of each POI is randomly chosen, $x \in [0, 1, 000]$, $y \in [0, 1, 000]$, and $z \in [0, 100]$. The importance weight w_j of each POI p_j in (2) is randomly chosen from an interval $[w_{\min}, w_{\max}]$, where a large weight w_j of POI p_j indicates that there are many people at p_j, $w_{\min} = 1$ and $w_{\max} = 1, 2, 5, 10, 15, 20$.

We employ a DJI Phantom 4 Pro UAV [25] to take photographs for POIs. Its battery capacity is $B = 5870$ mAh, and its longest flight time is $T = 30$ min $= 1800$ s when it is fully charged [25]. The UAV flies at a speed of $\vartheta = 10$ m/s. It hovers $\delta = 10$ s at each hovering position. The UAV is initially located at a corner of the area. The constant ξ in (1) is $\xi = 9.95$ by referring to the work in [15].

We evaluate the performance of the proposed algorithms against following four state-of-the-art algorithms.

1) The first algorithm `Greedy` schedules the UAV to collect the quality of photographs in a greedy way [35]. That is, the UAV visits hovering positions in decreasing order of the quality of photographs taken at each position, while ensuring that it has enough energy to return to the depot.
2) The second algorithm `IDIH` chooses the next to-be-visited POI with the minimum weighted sum of the distance from the UAV to the POI and the reciprocal of the POI importance weight [19].
3) The third algorithm `TopN` delivers a UAV flying tour by a hierarchical heuristic search algorithm [18].
4) The fourth algorithm `OP` reduces the problem to the orienteering problem, which is to find a flying tour with its total flying duration being no greater than T, such that the weighted sum of the importance weights of the POIs in the tour is maximized [29].

Each value in figures is the average result by applying each mentioned algorithm to 20 different network topologies with the same number of POIs. All experimental simulations were performed on a server with a 3.6 GHz CPU and an 8 GB memory.

B. Algorithm Performance in Real Network

We start by investigating the two proposed algorithms `ApproAlg` and `TreeAlg` against the four existing algorithms `OP`, `IDIH`, `Greedy`, and `TopN` in the network at Miami county, USA. Fig. 5(a) shows the distributions of the photograph qualities for different POIs in the flying tours delivered by different algorithms, where the photograph quality of a POI was defined in (2) in Section II-B, and the maximum photograph quality is no greater than 8. It can be seen from Fig. 5(a) that more than 66% of POIs in the photographs taken in the flying tours delivered by the existing algorithms have low photograph qualities that are less than 3, while no more than 57% of POIs by algorithms `ApproAlg` and `TreeAlg` have such low photograph qualities. For example, the percentages of POIs by algorithms `ApproAlg`, `TreeAlg`, `OP`, `IDIH`, `Greedy`, and `TopN` with a photograph quality less than 3 are 56%, 57%, 66%, 81%, 86%, and 83%, respectively. On the other hand, Fig. 5(a) demonstrates that about 14% and 9% of POIs by algorithms `ApproAlg` and `TreeAlg` have high photograph qualities greater than 6, whereas only 7% POIs by algorithm `OP` have such high qualities, and the percentages by algorithms `IDIH`, `Greedy`, and `TopN` are even no more than 1%.

Fig. 5(b) plots the total qualities of photographs taken in the flying tours delivered by different algorithms, which shows that the total quality by algorithm `ApproAlg` is the largest one among the six algorithms, and the total quality by algorithm `TreeAlg` is slightly less than that by algorithm `ApproAlg`. For example, the total qualities by algorithms `ApproAlg` and `TreeAlg` are about 11.5%($\approx$ (713−640/640)) and 8% ($\approx$ (692−640/640)) higher than that by algorithm `OP`. The rationale behind it is that more POIs by algorithms `ApproAlg` and `TreeAlg` have high photograph qualities than those by the existing algorithms, while less POIs by algorithms `ApproAlg` and `TreeAlg` have low qualities, see Fig. 5(a).

Fig. 5(c) illustrates that running time of algorithm `ApproAlg` is the maximum one, which is about 77 h, while the running times of the other five algorithms are no more than one second. Then, Fig. 5(c) implies that algorithm `ApproAlg` is not applicable to large networks. Also, Fig. 5(b) demonstrates that the total quality by the fast heuristic algorithm `TreeAlg` is only about 3% ($\approx$ (713 − 692/713)) less than that by algorithm `ApproAlg`, but its running time is only 0.05 s.

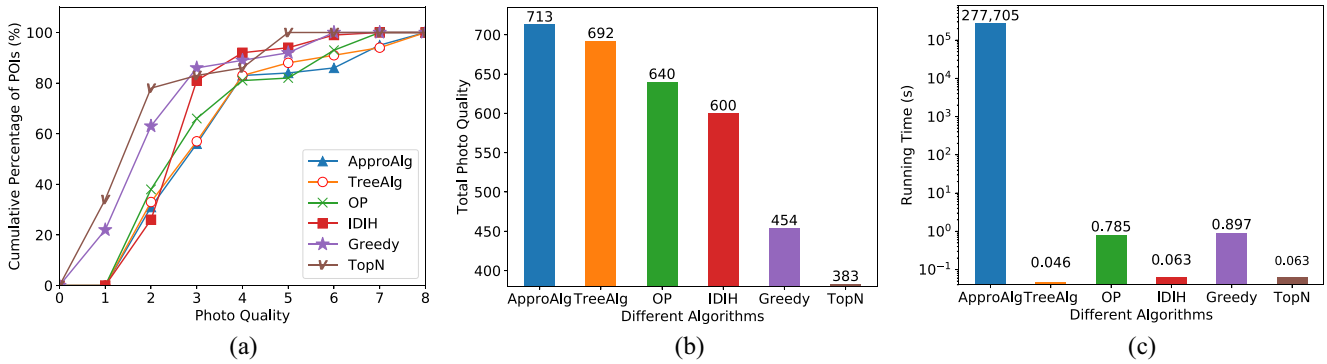

Fig. 5. Performance of different algorithms in the network at Miami county, USA, where $w_{\max} = 2$. (a) Distributions of the photograph qualities for different POIs by different algorithms. (b) Total photograph qualities by different algorithms. (c) Running times.

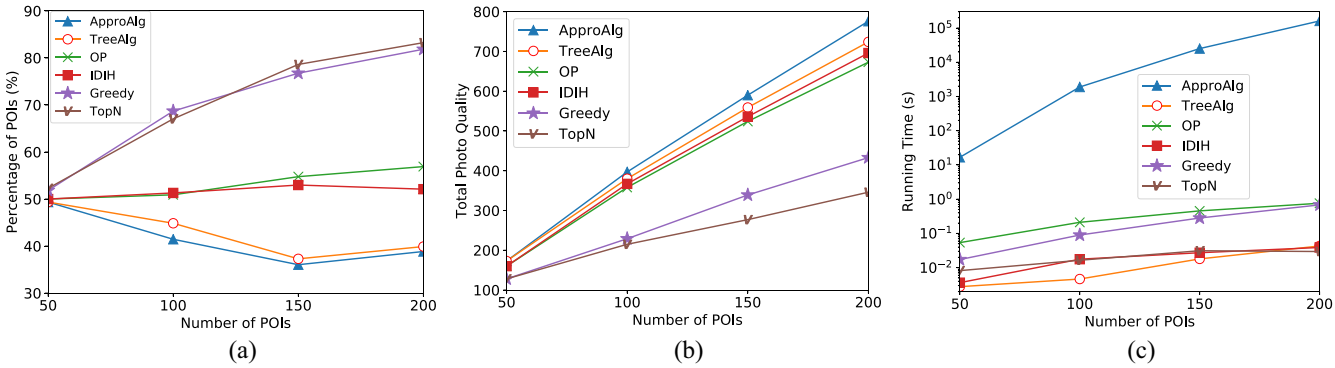

Fig. 6. The performance of different algorithms by varying the number of POIs from 50 to 200, where $w_{\max} = 2$. (a) Percentages of POIs with low photograph qualities less than 3. (b) Total photograph qualities by different algorithms. (c) Running time.

C. Algorithm Performance in Synthetic Networks

The rest is to evaluate the performance of different algorithms in synthetic networks. We first investigate the algorithm performance, by varying the number of POIs from 50 to 200. Fig. 6(a) shows that the percentages of POIs with low photograph qualities less than 3 by algorithms `ApproAlg` and `TreeAlg` are much smaller than those by the existing algorithms `OP`, `IDIH`, `Greedy`, and `TopN`. For example, the percentages of POIs with low photograph qualities by algorithms `ApproAlg`, `TreeAlg`, `OP`, `IDIH`, `Greedy`, and `TopN` are about 39%, 40%, 57%, 52%, 82%, and 83%, respectively, when there are 200 POIs. Fig. 6(b) demonstrates that the total photograph qualities by algorithms `ApproAlg` and `TreeAlg` are the top two among the six algorithms, e.g., about 15%($\approx (776-673/673)$) and 7.5% ($\approx (724-673/673)$) larger than those by the existing algorithms `OP`, `IDIH`, `Greedy`, and `TopN`, when there are 200 POIs. Fig. 6(b) plots the running times of different algorithms, where the running times of the five algorithms `TreeAlg`, `OP`, `IDIH`, `Greedy`, and `TopN` are no more than one second, whereas the running time of algorithm `ApproAlg` takes from 16 s to 44 h with the growth on the number of POIs from 50 to 200.

We then study the impact of the longest flying duration T of the UAV on the algorithm performance, by increasing T from 100 to 5000 s, when there are 100 POIs. It can be seen from Fig. 7(a) that the percentage of POIs with low photograph qualities by each of the mentioned algorithms decreases with a longer UAV flying duration T, as the UAV is able to visit more POIs if it can fly for a longer duration. Also, as depicted in Fig. 7(b), the total photograph quality by algorithm `ApproAlg` is the highest one among the six algorithms. It is interesting to see the total photograph quality by each of the four algorithms `ApproAlg`, `TreeAlg`, `OP`, and `IDIH` only slightly increases when the UAV flying duration T is longer than 3000 s. Furthermore, as shown in Fig. 7(c), the running time of algorithm `ApproAlg` significantly increases from 2.5 s to 35 min with the growth of T, while the running times of the other algorithms are much shorter than that by algorithm `ApproAlg`.

We also evaluate the impact of the flying speed ϑ of the UAV on the algorithm performance, by increasing the speed ϑ from 1 to 20 m/s, when there are 100 POIs and the longest UAV flying duration is $T = 1800$ s. It can be seen from Fig. 8 that the three curves by varying the UAV flying speed ϑ are similar to their corresponding curves in Fig. 7 by increasing the duration T. The rationale is that the UAV is able to visit more POIs if it can fly faster.

We further investigate the algorithm performance, by increasing the maximum POI weight $w_{\max}$ from 1 to 20, while fixing the minimum POI weight $w_{\min}$ at 1, i.e., $w_{\min} = 1$, where the weight w_j of POI p_j is randomly chosen from $[w_{\min}, w_{\max}]$, and a large weight w_j implies that there are many people at POI p_j. Recall that we defined that a POI p_j has a low photograph quality if the amount of nonredundant

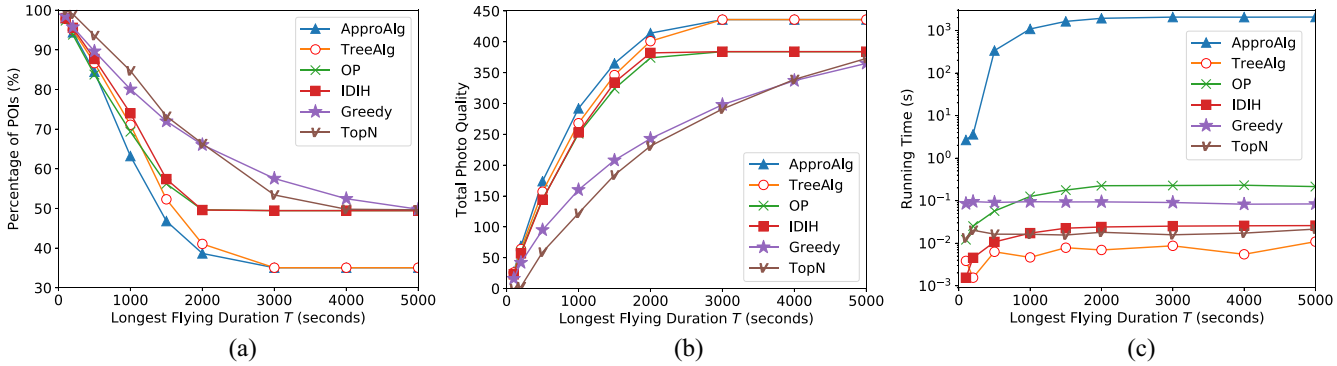

Fig. 7. Performance of different algorithms by increasing the longest flying duration T of the UAV from 100 to 5,000 s, when there are 100 POIs and $w_{\max} = 2$. (a) Percentages of POIs with low photograph qualities less than 3. (b) Total photograph qualities by different algorithms. (c) Running times.

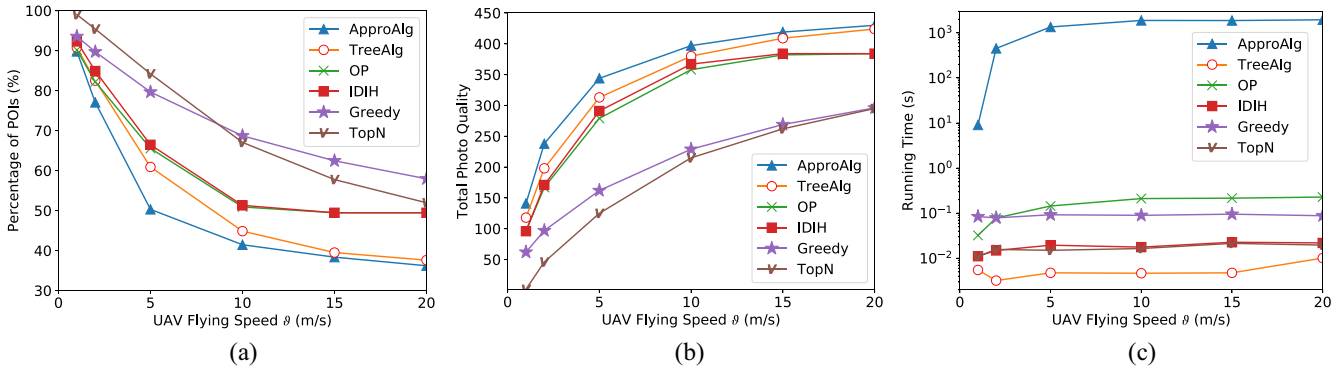

Fig. 8. Performance of different algorithms by increasing the flying speed ϑ of the UAV from 1 to 20 m/s, when there are 100 POIs, $T = 1800$, and $w_{\max} = 2$. (a) Percentages of POIs with low photograph qualities less than 3. (b) Total photograph qualities by different algorithms. (c) Running times.

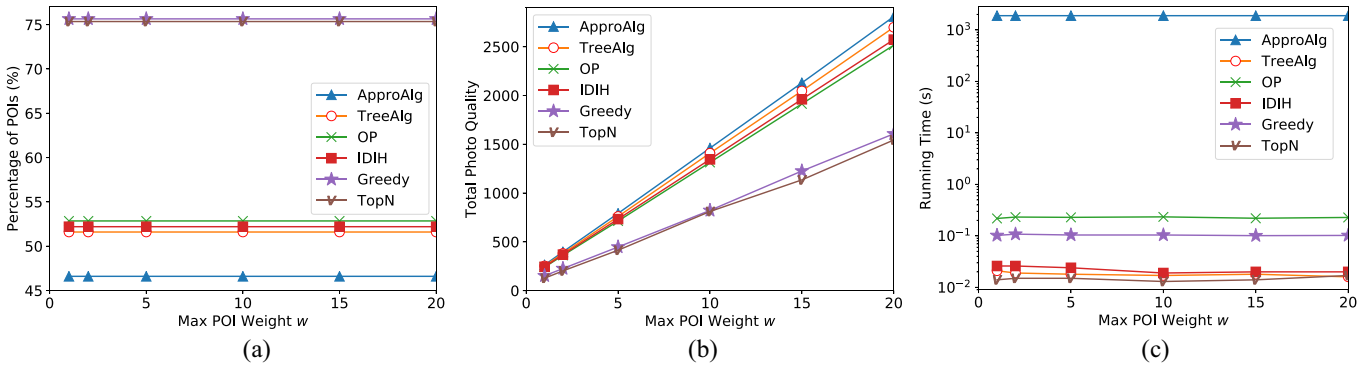

Fig. 9. Performance of different algorithms by increasing the maximum POI weight $w_{\max}$ from 1 to 20, when there are 100 POIs, $T = 1800$ s, and $w_{\min} = 1$. (a) Percentages of POIs with low photograph qualities. (b) Total photograph qualities by different algorithms. (c) Running times.

information f_j collected for the POI is no more than 3 when the maximum POI weight $w_{\max} = 2$, i.e., $f_j \leq 3$, see Figs. 5(a), 6(a), 7(a), and 8(a). However, the value of f_j is proportional to the maximum POI weight $w_{\max}$, see (2) and (3) in Section II-B. Notice that the average POI weight is $[(w_{\min} + w_{\max})/2] = (1 + 2/2) = 1.5$ when $w_{\max} = 2$. For any value of $w_{\max}$, we thus define that a POI p_j has low photograph qualities if the value of f_j is no more than $f_{\text{low}} = 3 \cdot [((w_{\min} + w_{\max})/2)/1.5] = w_{\min} + w_{\max}$, i.e., $f_j \leq f_{\text{low}} = 1w_{\min} + w_{\max}$. It can be seen that when $w_{\max} = 2$, $f_{\text{low}} = 1 + 2 = 3$. Fig. 9(a) plots that the percentage of POIs with low photograph qualities by each algorithm almost does not change with the growth of $w_{\max}$, as the low photograph quality threshold f_{low} is proportional to $w_{\max}$. Fig. 9(b) shows that the total photograph quality by each algorithm increases with a larger value of $w_{\max}$, and the total photograph qualities by algorithms `ApproAlg` and `TreeAlg` are at least 9% ($\approx (2809 - 2577/2577)$) and 5% ($\approx (2699 - 2577/2577)$) larger than those by the other algorithms, respectively. Fig. 9(c) demonstrates that the running time by each algorithm also does not change with the increase of $w_{\max}$.

We finally study the tradeoff between the algorithm performance and the algorithm running time, by varying the scaling coefficient ϵ in the approximation algorithm `ApproAlg` from 0.1 to 1. Following Lemma 4 and Theorem 1 in Section III-C, the performance of the approximation

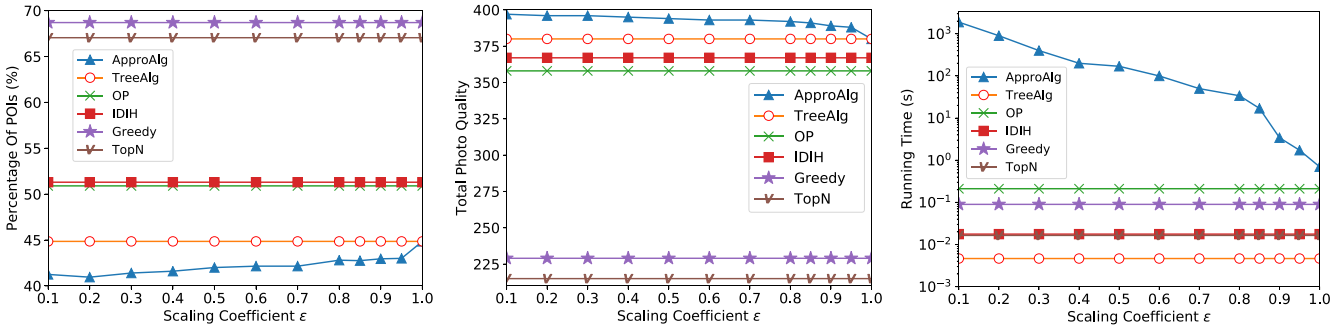

Fig. 10. Tradeoff between the performance of algorithm ApproAlg and its running time, by increasing the scaling coefficient ϵ from 0.1 to 1, when there are 100 POIs and $T = 1800$ s. (a) Percentages of POIs with low photograph qualities. (b) Total photograph qualities by different algorithms. (c) Running times.

algorithm is better if the value of ϵ is smaller, but its running time will become longer. In contrast, the algorithm runs faster with a larger value of ϵ, whereas its performance decreases. Fig. 10(a) and (b) shows that the performance of algorithm ApproAlg gradually deceases with the increase of ϵ, while Fig. 10(c) plots that the running time of algorithm ApproAlg decreases from about a half hour to only about one second. It must be emphasized that the choice of an appropriate value of ϵ depends on the application requirement of the disaster relief. That is, if it is only for a short period, e.g., a few minutes, is allowed to find a UAV flying tour, a larger value of ϵ must be adopted or a more powerful server, e.g., a supercomputer, must be deployed to execute the algorithm. On the other hand, if the disaster relief can tolerate a few hours of delay, a smaller value of ϵ can be adopted in order to find a better flying tour.

It can be seen from Figs. 6–10 that the two proposed algorithms ApproAlg and TreeAlg perform much better than the four benchmarks OP, IDIH, Greedy, and TopN in terms of the total photograph qualities. This indicates that the UAV in the identified flying tours by the former two algorithms can collect more valuable nonredundant information for rescue decision-making, and the people trapped in a disaster area may be rescued earlier. On the other hand, the running time of algorithm ApproAlg is high, while the heuristic algorithm TreeAlg runs much faster, whereas its performance is only slightly worse than that by algorithm ApproAlg.

VI. Related Work

Extensive studies have been conducted for the deployment of UAVs for information collection of points of interest. Several studies focused on the problem of dispatching one UAV or a fleet of UAVs to cover a monitoring area, assuming that each UAV has an unlimited energy supply [21], [30], [35], [42], among which some investigated the problem of fully covering a target area by UAVs, so as to minimize the cost consumption of dispatching the UAVs (e.g., the cost is the number of dispatched UAVs or their total energy consumption) [21], [30], [42]. For example, Torres *et al.* [30] investigated the problem of finding a flying tour for a UAV to fully cover an area of interest with the minimum energy consumption of the UAV. They proposed an algorithm to obtain a minimum energy consumption flying tour, by minimizing the number of turns during the tour. Modares *et al.* [21] extended the single UAV case in [30] to the case of a fleet of UAVs, and proposed a heuristic algorithm for tour planning, which takes into account the flying distance and number of turns during flying. Zorbas *et al.* [42] assumed that the higher a UAV flies, the larger area it covers, and more energy it consumes. They studied the problem of finding an optimal placement of multiple UAVs to fully cover an area, so as to minimize the total cost. On the other hand, Wang *et al.* [35] investigated the problem of maximizing the information collected by a fleet of UAVs. They proposed a fog-networking architecture system to coordinate multiple UAVs for capturing mobile points of interest in a football game.

Unlike those studies in [21], [30], [35], and [42] that assumed each UAV has an unlimited energy supply, other studies did consider the energy capacity constraint on each UAV [18], [19], [27], [29], [31]. For example, Lin and Goodrich [18] investigated the problem of finding a flying tour for a UAV to maximize the probability of finding a missing person, within a given flying duration. Tokekar *et al.* [29] studied the problem of dispatching a UAV and an unmanned ground vehicle to collect information about soil nitrogen levels in precision agriculture, by reducing the problem to the orienteering problem. Scott *et al.* [27] extended the work in [30] by considering the constrained energy capacity of the UAV. Mersheeva and Friedrich [19] introduced a monitoring problem that employs a fleet of UAVs to take photographs for POIs periodically in a disaster area, assuming that different POIs have different priorities. Trotta *et al.* [31] assumed that UAVs can recharge their batteries at stations on the ground. They proposed a distributed, bio-inspired algorithm to find an optimal charging scheduling and flying tour for UAVs to cover an area, such that the network lifetime is maximized.

We also notice that there are some studies on transmission energy saving of mobile devices [13], [16], [17], [28], [41]. Specifically, Liu *et al.* [17] are ones of the pioneers of introducing cloud computing to assist mobile devices to gather, store and process data, and they also discussed the challenges, such as energy-efficient interactions, virtual machine migration overhead, privacy, and security. Then they studied the problem

of energy-efficient transmission between mobile devices and cloud platforms, so as to minimize the energy consumption of mobile devices under delay constraints, by adaptively prefetching frequently used data when the down-link channel is in good condition, while deferring the transmission of delay-tolerant data with bad channel condition [16], [28]. Jin *et al.* [13] recognized that the frequent heart messages of Instant Message APPs in smartphones are very energy consuming, and proposed a device-to-device (D2D)-based heartbeat relaying framework, which selects energy-sufficient smartphones as relays to opportunistically collect heartbeat messages from nearby smartphones using energy-efficient D2D communication, and then transmitted to the BS in an aggregated manner. Zhang *et al.* [41] further reduced energy consumption of smartphones by piggybacking aggregated delay-tolerant data with heartbeat messages, so as to minimize the cumulative tail energy incurred by heartbeat messages. We noted that the algorithms in these studies cannot be applicable to the monitoring quality maximization problem in this paper, since they assumed that data is independent, while in this paper the photographs taken by a UAV at nearby locations usually overlap with each other.

In this paper we studied the problem of employing a UAV to collect the maximum nonredundant information of POIs by taking photographs for them. We incorporated not only the limited UAV energy capacity but also the redundant information of multiple photographs taken at nearby locations. We developed a novel approximation algorithm and a fast heuristic algorithm for the problem.

VII. Conclusion

In this paper we studied the use of a UAV to take photographs for POIs in a disaster region, with the aim to maximize the accumulative photograph quality collected by the UAV, subject to the limited energy capacity on the UAV. We first modeled the photograph quality by a submodular function, and formulated a novel monitoring quality maximization problem. Due to NP-hardness of the problem, we then proposed an $O(\log n)$-approximation algorithm with quasi-polynomial time complexity. We also devised a fast yet scalable heuristic algorithm for the problem. We finally evaluated the performance of the proposed algorithms on both a real and synthetic networks through extensive simulations. Experimental results showed that the proposed algorithms are very promising. Especially, the amounts of nonredundant information by the proposed approximation and heuristic algorithms are about 11% and 8% more than that by the state-of-the-art, respectively. To the best of our knowledge, we are the first to consider the novel problem of collecting quality information with an energy-constrained UAV.

References

[1] C. A. B. Baker, S. Ramchurn, W. T. L. Teacy, and N. R. Jennings, "Planning search and rescue missions for UAV teams," in *Proc. Eur. Conf. Artif. Intell. (ECAI)*, 2017, pp. 1777–1782.

[2] G. Bevacqua, J. Cacace, A. Finzi, and V. Lippiello, "Mixed-initiative planning and execution for multiple drones in search and rescue missions," in *Proc. 25th Int. Conf. Autom. Plan. Scheduling*, 2015, pp. 315–323.

[3] H. Y. Chao *et al.*, "Band-reconfigurable multi-UAV-based cooperative remote sensing for real-time water management and distributed irrigation control," in *Proc. 17th World Congr. Int. Feder. Autom. Control (IFAC)*, 2008, pp. 11744–11749.

[4] C. Chekuri and M. Pál, "A recursive greedy algorithm for walks in direct graphs," in *Proc. 46th Annu. IEEE Symp. Found. Comput. Sci. (FOCS)*, 2005, pp. 245–253.

[5] S. Chessa *et al.*, "Sensing the cities with social-aware unmanned aerial vehicles," in *Proc. IEEE Symp. Comput. Commun.*, 2017, pp. 278–283.

[6] (2017). *Drone Using in Hurricane IRMA*. [Online]. Available: http://thedronegirl.com/2017/09/16/7-ways-drones-helping-hurricane-irma-harvey-recovery-experts/

[7] M. Erdelj, E. Natalizio, K. R. Natalizio, and I. F. Akyildiz, "Help from the sky: Leveraging UAVs for disaster management," *IEEE Pervasive Comput.*, vol. 16, no. 1, pp. 24–32, Jan./Mar. 2017.

[8] B. L. Golden, L. Levy, and R. Vohra, "The orienteering problem," *Naval Res. Logist.*, vol. 34, no. 3, pp. 307–318, 1987.

[9] Q. Guo *et al.*, "Towards low-cost yet high-performance sensor networks by deploying a few ultra-fast battery powered sensors," *Sensors*, vol. 18, no. 9, p. 2771, 2018.

[10] S. Hayat, E. Yanmaz, T. X. Brown, and C. Bettstetter, "Multi-objective UAV path planning for search and rescue," in *Proc. IEEE Int. Conf. Robot. Autom. (ICRA)*, 2017, pp. 5569–5574.

[11] C. S. Hua, J. T. Qi, H. Shang, W. J. Hu, and J. D. Han, "Detection of collapsed building with the aerial images captured from UAV," *Sci. China Inf. Sci.*, vol. 59, no. 3, pp. 1–15, 2016.

[12] Z. C. Huang and T. Zhu, "Distributed real-time multimodal data forwarding in unmanned aerial systems," in *Proc. 14th Annu. IEEE Int. Conf. Sens. Commun. Netw. (SECON)*, 2017, pp. 1–9.

[13] Y. Jin, F. Liu, X. Yi, and M. Chen, "Reducing cellular signaling traffic for heartbeat messages via energy-efficient D2D forwarding," in *Proc. IEEE 37th Int. Conf. Distrib. Comput. Syst. (ICDCS)*, 2017, pp. 1301–1311.

[14] A. Kleiner and A. Kolling, "Guaranteed search with large teams of unmanned aerial vehicles," in *Proc. IEEE Int. Conf. Robot. Autom. (ICRA)*, 2013, pp. 2977–2983.

[15] J. Lee and S. Sung, "Evaluating spatial resolution for quality assurance of UAV images," *Spat. Inf. Res.*, vol. 24, no. 2, pp. 141–154, 2016.

[16] F. Liu, P. Shu, and J. C. S. Lui, "AppATP: An energy conserving adaptive mobile-cloud transmission protocol," *IEEE Trans. Comput.*, vol. 64, no. 11, pp. 3051–3063, Nov. 2015.

[17] F. Liu *et al.*, "Gearing resource-poor mobile devices with powerful clouds: Architectures, challenges, and applications," *IEEE Wireless Commun.*, vol. 20, no. 3, pp. 14–22, Jun. 2013.

[18] L. Lin and M. A. Goodrich, "Hierarchical heuristic search using a Gaussian mixture model for UAV coverage planning," *IEEE Trans. Cybern.*, vol. 44, no. 12, pp. 2532–2544, Dec. 2014.

[19] V. Mersheeva and G. Friedrich, "Multi-UAV monitoring with priorities and limited energy resources," in *Proc. 25th Conf. Autom. Plan. Scheduling*, 2015, pp. 327–356.

[20] S. Milani and A. Memo, "Impact of drone swarm formations in 3D reconstruction," in *Proc. IEEE Int. Conf. Image Process. (ICIP)*, 2016, pp. 2598–2602.

[21] J. Modares, F. Ghanei, N. Mastronarde, and K. Dantu, "UB-ANC planner: Energy efficient coverage path planning with multiple drones," in *Proc. IEEE Conf. Robot. Autom.*, 2017, pp. 6182–6189.

[22] J. Modares, N. Mastronarde, and K. Dantu, "UB-ANC emulator: An emulation framework for multiagent drone networks," in *Proc. IEEE Int. Conf. Simulat. Model. Program. Auton. Robots (SIMPAR)*, 2016, pp. 252–258.

[23] S. Naqvi *et al.*, "Energy efficiency analysis of UAV-assisted mmWave HetNets," in *Proc. IEEE Int. Conf. Commun. (ICC)*, May 2018, pp. 1–6.

[24] L. Paull, C. Thibault, A. Nagaty, M. Seto, and H. Li, "Sensor-driven area coverage for an autonomous fixed-wing unmanned aerial vehicle," *IEEE Trans. Cybern.*, vol. 44, no. 9, pp. 1605–1618, Sep. 2014.

[25] (2017). *Phantom 4 Specification*. [Online]. Available: https://www.dji.com/phantom-4-adv/info

[26] L. D. P. Pugliese, F. Guerriero, D. Zorbas, and T. Razafindralambo, "Modelling the mobile target covering problem using flying drones," *Optim. Lett.*, vol. 10, no. 5, pp. 1021–1052, 2016.

[27] K. Scott, R. Dai, and M. Kumar, "Occlusion-aware coverage for efficient visual sensing in unmanned aerial vehicle networks," in *Proc. IEEE Glob. Commun. Conf. (GLOBECOM)*, 2016, pp. 1–6.

[28] P. Shu *et al.*, "eTime: Energy-efficient transmission between cloud and mobile devices," in *Proc. 32nd IEEE Int. Conf. Comput. Commun.*, 2013, pp. 195–199.

[29] P. Tokekar, J. V. Hook, D. Mulla, and V. Isler, "Sensor planning for a symbiotic UAV and UGV system for precision agriculture," *IEEE Trans. Robot.*, vol. 32, no. 6, pp. 1498–1511, Dec. 2016.
[30] M. Torres, D. A. Pelta, J. L. Verdegay, and J. C. Torres, "Coverage path planning with unmanned aerial vehicles for 3D terrain reconstruction," *Exp. Syst. Appl.*, vol. 55, no. 15, pp. 441–451, Aug. 2015.
[31] A. Trotta, M. D. Felice, K. R. Chowdhury, and L. Bononi, "Fly and recharge: Achieving persistent coverage using small unmanned aerial vehicles (SUAVs)," in *Proc. IEEE Int. Conf. Commun. (ICC)*, 2017, pp. 1–7.
[32] P. Vansteenwegen, W. Souffriau, and D. V. Oudheusden, "The orienteering problem: A survey," *Eur. J. Oper. Res.*, vol. 209, no. 1, pp. 1–10, 2011.
[33] V. V. Vazirani, *Approximation Algorithms*. Heidelberg, Germany: Springer, 2003.
[34] A. Wallar, E. Plaku, and D. A. Sofge, "Reactive motion planning for unmanned aerial surveillance of risk-sensitive areas," *IEEE Trans. Autom. Sci. Eng.*, vol. 12, no. 3, pp. 969–989, Jul. 2015.
[35] X. L. Wang, A. Chowdhery, and M. Chiang, "Networked drone cameras for sports streaming," in *Proc. IEEE 37th Conf. Distrib. Comput. Syst. (ICDCS)*, 2017, pp. 308–318.
[36] D. Wu *et al.*, "ADDSEN: Adaptive data processing and dissemination for drone swarms in urban sensing," *IEEE Trans. Comput.*, vol. 66, no. 2, pp. 183–198, Feb. 2017.
[37] W. Xu *et al.*, "Maximizing sensor lifetime with the minimal service cost of a mobile charger in wireless sensor networks," *IEEE Trans. Mobile Comput.*, vol. 17, no. 11, pp. 2564–2577, Nov. 2018.
[38] W. Xu, W. Liang, X. Lin, and G. Mao, "Efficient scheduling of multiple mobile chargers for wireless sensor networks," *IEEE Trans. Veh. Technol.*, vol. 65, no. 9, pp. 7670–7683, Sep. 2016.
[39] J. Xu, G. Solmaz, R. Rahmatizadeh, D. Turgut, and L. Bölöni, "Animal monitoring with unmanned aerial vehicle-aided wireless sensor networks," in *Proc. IEEE 40th Conf. Local Comput. Netw. (LCN)*, 2015, pp. 125–132.
[40] Q. Zhang *et al.*, "An improved algorithm for dispatching the minimum number of electric charging vehicles for wireless sensor networks," *Wireless Netw.*, pp. 1–14, May 2018. [Online]. Available: https://link.springer.com/article/10.1007%2Fs11276-018-1765-5
[41] T. Zhang *et al.*, "eTrain: Making wasted energy useful by utilizing heartbeats for mobile data transmissions," in *Proc. IEEE 35th Int. Conf. Distrib. Comput. Syst. (ICDCS)*, 2015, pp. 113–122.
[42] D. Zorbas, L. D. P. Pugliese, T. Razafindralambo, and F. Guerriero, "Optimal drone placement and cost-efficient target coverage," *J. Netw. Comput. Appl.*, vol. 75, pp. 16–31, Nov. 2016.
[43] D. Zorbas, T. Razafindralambo, D. P. P. Luigi, and F. Guerriero, "Energy efficient mobile target tracking using flying drones," in *Proc. 4th Int. Conf. Ambient Syst. Netw. Technol.*, 2013, pp. 80–87.
[44] T. Zou *et al.*, "Improving charging capacity for wireless sensor networks by deploying one mobile vehicle with multiple removable chargers," *Ad Hoc Netw.*, vol. 63, pp. 79–90, Aug. 2017.

Yan Liang received the B.Sc. degree in computer science from Sichuan University, Chengdu, China, in 2016, where she is currently pursuing the master's degree in computer science.

Her current research interests include mobile computing, wireless sensor networks, and graph theory.

Wenzheng Xu (M'15) received the B.Sc., M.E., and Ph.D. degrees in computer science from Sun Yat-sen University, Guangzhou, China, in 2008, 2010, and 2015, respectively.

He is currently an Associate Professor with Sichuan University, Chengdu, China. He was a Visitor with Australian National University, Canberra, ACT, Australia, and the Chinese University of Hong Kong, Hong Kong. His current research interests include wireless ad hoc and sensor networks, online social networks, mobile computing, approximation algorithms, combinatorial optimization, and graph theory.

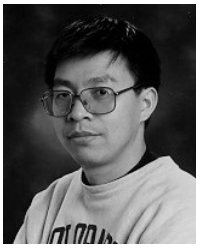

Weifa Liang (M'99–SM'01) received the B.Sc. degree in computer science from Wuhan University, Wuhan, China, in 1984, the M.E. degree in computer science from the University of Science and Technology of China, Hefei, China, in 1989, and the Ph.D. degree in computer science from Australian National University, Canberra, ACT, Australia, in 1998.

He is currently a Professor with Australian National University. His current research interests include wireless ad hoc and sensor networks, cloud computing, software-defined networking, online social networks, design and analysis of parallel and distributed algorithms, approximation algorithms, combinatorial optimization, and graph theory.

Jian Peng received the B.A. and Ph.D. degrees from the University of Electronic Science and Technology of China, Chengdu, China, in 1992 and 2004, respectively.

He is a Professor with the College of Computer Science, Sichuan University, Chengdu, China. His current research interests include big data, wireless sensor networks, and cloud computing.

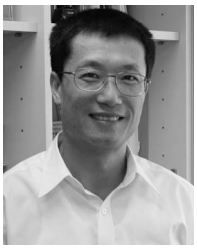

Xiaohua Jia (A'00–SM'01–F'13) received the B.Sc. and M.Eng. degrees from the University of Science and Technology of China, Hefei, China, in 1984 and 1987, respectively, and the D.Sc. degree in information science from the University of Tokyo, Tokyo, Japan, in 1991.

He is currently a Chair Professor with the Department of Computer Science, City University of Hong Kong, Hong Kong. His current research interests include cloud computing and distributed systems, computer networks, wireless sensor networks, and mobile wireless networks.

Dr. Jia is an Editor of the IEEE TRANSACTIONS ON PARALLEL AND DISTRIBUTED SYSTEMS from 2006 to 2009 and the *Journal of World Wide Web*. He is the General Chair of ACM MobiHoc 2008, the TPC Co-Chair of IEEE MASS 2009, the Area-Chair of IEEE INFOCOM 2010, and the Panel Co-Chair of IEEE INFOCOM 2011.

Yingjie Zhou (M'14) received the Ph.D. degree from the School of Communication and Information Engineering, University of Electronic Science and Technology of China, Chengdu, China, in 2013.

He is currently an Assistant Professor with the College of Computer Science, Sichuan University, Chengdu. He was a Visiting Scholar with the Department of Electrical Engineering, Columbia University, New York, NY, USA. His current research interests include network measurement, behavioral data analysis, resource allocation, and neural networks.

Lei Duan received the B.Sc. and Ph.D. degrees in computer science from Sichuan University, Chengdu, China, in 2003 and 2008, respectively. He is currently pursuing the Ph.D. degree at the Department of Computer Science and Engineering, Wright State University, Dayton, OH, USA, in 2008.

He is currently a Professor with the School of Computer Science, Sichuan University. He was a Visiting Scholar with the School of Computing Science, Simon Fraser University, Burnaby, BC, Canada, from 2012 to 2013. His current research interests include data mining, knowledge management, evolutionary computation, bioinformatics, and health-informatics.